Journal of Applied Mechanics and Technical Physics, Vol. 46, No. 6, pp. 867–875, 2005

SOIL BEHAVIOR AT THE INTERFACE WITH A RIGID PROJECTILE DURING PENETRATION

V. A. Veldanov and S. V. Fedorov

UDC 531.58

The motion and state of soil at the interface with a penetrating rigid projectile is studied by numerical solution of the problem of a cylindrical projectile which expands and at the same time moves translationally along its axis in soil. The soil behavior is described using the model of a compressible elastoplastic medium with transition to a plastic state depending on the pressure in it. It is shown that a thin layer of soil at the interface with the projectile nose should be set in motion and move together with the projectile without sliding. An analysis is performed of the validity of using the dry friction law to determine the shear stresses on the projectile surface during penetration. The heat release in the soil layer at the interface due to internal friction and its possible effect on the penetration are estimated.

Key words: *soil, rigid projectile, penetration, friction, heat release.*

Introduction. The dynamics of projectile penetration into soils depends greatly on the features of motion and state of the soil material at the interface with the projectile. The soil behavior in this region influences the distributions of normal and tangential mechanical stresses on the projectile surface, which determines the dynamic effect on the projectile during motion in the soil.

For metal projectiles penetrating into soil targets (STs) at velocities of up to 1000 m/sec, the strains of the projectiles are small [1] and they can be treated as absolutely rigid bodies (Fig. 1). The penetration of rigid projectiles into STs is frequently calculated using assumptions on a particular nature of motion of soil particles near the interface with the projectile nose. Such assumptions considerably simplify the solution of the problem and in many cases allow one to describe the motion dynamics of projectiles in STs in finite analytical form. In penetration problems, the motion of thin pointed projectiles in soil (for projectiles with conical noses, the cone angle 2γ as a rule does not exceed 30°) is usually calculated using the hypothesis of plane cross sections and the penetration of blunt nosed projectiles using the hypothesis of normal trajectories [2]. The first hypothesis assumes that during penetration, the soil particles move in a straight line normal to the projectile axis, and according to the second hypothesis, the soil particle trajectories normal to the surface of the projectile nose. The hypotheses of plane cross section and normal trajectories allow one to describe the rectilinear motion of soil particles from the projectile in a one-dimensional approximation and to determine the normal stresses σ_n acting on the projectile surface in contact with soil. Next, the shear stresses τ_n on the surface of the projectile nose are usually calculated using the dry friction law:

$$\tau_n = \mu\sigma_n, \tag{1}$$

where μ is the friction coefficient [2]. The dry friction law is often used to determine the shear stresses on the surface of a rigid projectile and in penetration models of higher levels based on numerical integration of the general system of equations of continuum mechanics [3]. In this case, however, the use of relation $\tau_n = \mu\sigma_n$ can involve physical inconsistencies and in many cases is unjustified. One of the inconsistencies is that the shear stresses (which act not

Bauman Moscow State Technical University, Moscow 105005; sm4@sm.bmstu.ru. Translated from Prikladnaya Mekhanika i Tekhnicheskaya Fizika, Vol. 46, No. 6, pp. 116–127, November–December, 2005. Original article submitted January 20, 2004; revision submitted December 29, 2004.

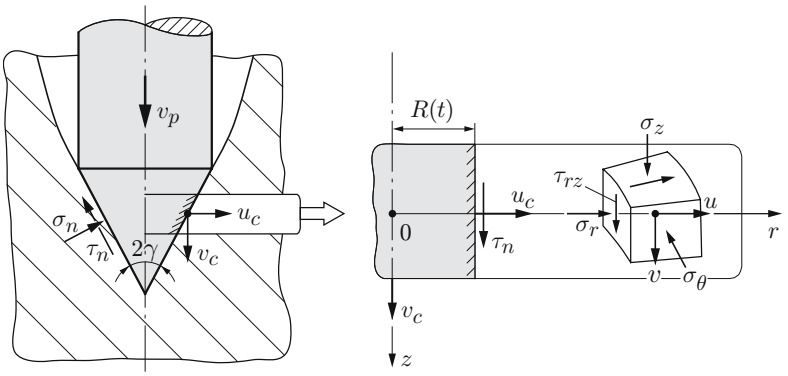

Fig. 1. Calculated diagram of interaction of a rigid projectile with a soil target.

only on the projectile but also on the soil at the interface with the projectile) calculated using the dry frictions law can considerably surpass the strength properties of the soil. The models of plastic or elastoplastic media, which are mainly employed to describe soil behavior under dynamic loading, ignore the action of such shear stresses in the medium [4, 5]. To illustrate the indicated circumstance, we estimate the contact shear stresses (1) using empirical resistance laws [6] that relate the normal stresses σ_n on the projectile surface to the projection v_n of the velocity of a given point of the surface onto the normal to the surface. We use the resistance law

$$\sigma_n = Av_n^2 + C, \tag{2}$$

where A and C are empirical coefficients that depend on soil properties [6]. For a conical-nose projectile, the velocity component $v_n = v_p \sin\gamma$, where v_p is the projectile velocity and γ is the cone half-angle. For a projectile with a cone angle $2\gamma = 60^\circ$ penetrating at a velocity $v_p = 500$ m/sec, for example, into a dense soil ($A = 1900$ kg/m^3 and $C = 10$ MPa), we obtain $\sigma_n \approx 130$ MPa. For soils, the coefficient of skin friction μ of soil on metal varies from 0.2 to 0.6 [7]. Then, for the case considered, relation (1) even for minimum values of μ gives shear stresses in the soil at the interface with the projectile that exceed the shear strength of the soil by at least a factor of three [5].

Anther contradictory result is obtained in an attempt to estimate the heat release on the projectile–soil interface [8]. The dry friction law assumes sliding of the soil particles at the interface with the projectile and, hence, a frictional heat-release mechanism at this boundary (due to mechanical-energy dissipation by sliding friction at the projectile–soil interface) [9].

The frictional-heating rate can still be estimated using the empirical resistance law (2). In the calculation of τ_n using formula (1), the heat flux q on the surface of the conical nose of the projectile due to skin friction (the energy released from the unit area of the interface in unit time) is defined as

$$q = \tau_n v_\tau = \mu\sigma_n v_\tau,$$

where v_τ is the velocity of sliding of soil particles along the cone surface. Using the hypothesis of normal trajectories [2] (the soil particles move normal to the cone surface), we assume that the sliding velocity $v_\tau = v_p \cos\gamma$. Then, the expression for the heat flux taking into account (2) becomes

$$q = \mu(Av_p^2 \sin^2\gamma + C)v_p \cos\gamma. \tag{3}$$

According to the above relation, at a penetration velocity of a few hundred meters per second, the heat-release rate at the projectile–soil interface can reach about 10 GW/m^2 (which is approximately 10^3 times higher than the heat fluxes that arise on the walls of a jet engine nozzles during combustion gas exhaust [10]). The strength properties of the soil have an insignificant effect on the value of the heat flux (3) at penetration velocities over 500 m/sec [at such velocities, the contact stresses (2), which influences the heat-release rate, are determined primarily by the inertial component of the resistance forces]. As a result, the frictional-heating rate depends strongly on the penetration velocity [according to (3), the heat flux increases in proportion to the cube of the penetration velocity].

The temperatures to which the penetrating projectile material can be heated by skin friction are estimated by solving the heat-conduction equation for the half-space on whose boundary the constant heat flux q is specified [11].

According to this solution, the temperature T_s of the boundary of the half-space increases with time t under the law

$$T_s = 2q\sqrt{t}\,/\sqrt{\pi\lambda_m c_m \rho_m},$$

where λ_m is the thermal conductivity, c_m is the specific heat, and ρ_m is the material density (the thermal characteristics correspond to the projectile material). The estimates of [8] show that the heat fluxes due to the frictional heating mechanism can increase the projectile surface temperature by a few thousand degrees in a few microseconds, which is smaller than the penetration time. The fast heating of the near-surface layers of the projectile is due to two factors: 1) the very powerful heat flux (3) that arises from the friction at the interface with the soil; 2) the impossibility of fast removal of the released heat into the interior of the projectile material. The heat-conduction rate is far slower than the rate of heat transfer from the projectile surface even for metals with the highest thermal conductivities. Accounting for the fact that the heat released at the interface heats not only the projectile but also the soil [9] does not significantly change the above estimates (the order of magnitude of the heat fluxes affecting the projectile remains unchanged).

Thus, the above estimates show that even for rather low penetration velocities (a few hundred meters per second), the heating of the projectile due to frictional heat-release should inevitably result in the thermal destruction and ablation (due to melting and chemical erosion) of the projectile surface layer in contact with soil. As a result, the shape of the projectile nose and its weight should change significantly during penetration. However, in experiments these effects have not observed up to penetration velocities of 500 m/sec [1].

Model for Projectile Penetration into Soil. The foregoing implies that there is an urgent need for a detailed study of the contact interaction during projectile penetration into STs. To obtain computational–theoretical estimates of the parameters of motion and state of soil at the interface with a moving projectile, as a first approximation we can use the simplified quasi-dimensional model described below. Let us consider an infinitely long cylindrical piston which expands at a specified constant velocity u_c in an unbounded medium and simultaneously performs translational motion along the axis at a constant velocity v_c (see Fig. 1). Obviously, the motion of the soil due to the penetration of the piston has rotational symmetry; furthermore, because of the friction at the interface with the piston, the soil particles have both radial and axial velocity components. The stress state of the soil is characterized by a stress tensor with three normal components (axial σ_z, radial σ_r, and tangential σ_θ) and with one shear stress τ_{rz} (see Fig. 1). All parameters of motion and state of the medium depend only on one spatial coordinate, which is reckoned in the radial direction.

Setting a definite ratio of the kinematic parameters of the piston v_c and u_c in the problem considered, it is possible to approximately model the effect exerted on soil by rigid projectiles with various nose cone angles at various penetration velocities. In this case, the axial velocity of the piston v_c is considered the penetration velocity, and for the specified value of v_c, the radial velocity of expansion of the piston u_c should be defined as a function of the cone half-angle γ of the projectile nose $u_c = v_c \tan\gamma$. We note that this definition of the velocity u_c corresponds to the hypothesis of plane cross sections [2], which is used to calculate the penetration of thin pointed projectiles into STs. However, unlike in this hypothesis, which postulates only radial motion of the entire medium, in the model considered, the soil particle can move in both the radial and axial directions.

In cylindrical coordinates (r, z), the motion of the medium in the radial and axial directions with allowance for the independence of the determining parameters on the z coordinate is described by the equations

$$\rho\frac{du}{dt} = \frac{\partial\sigma_r}{\partial r} + \frac{\sigma_r - \sigma_\theta}{r}, \qquad \rho\frac{dv}{dt} = \frac{\partial\tau_{rz}}{\partial r} + \frac{\tau_{rz}}{r},$$

where u and v are the radial and axial velocity components of the soil particles, respectively and ρ is the soil density.

To determine the stresses that arise in the ST material, we use the model of a compressible elastoplastic medium. This model has been extensively used in numerical solutions of penetration problems for soil–concrete media [3, 12] since it takes into account the main properties of such media related to their considerable volumetric compressibility and capability to resist shear deformation. In the problem considered, the variation in the ST density is given by the continuity equation

$$\frac{1}{\rho}\frac{d\rho}{dt} + \dot{\varepsilon}_r + \dot{\varepsilon}_\theta = 0,$$

where $\dot{\varepsilon}_r$ and $\dot{\varepsilon}_\theta$ are the radial and shear components of the strain-rate tensor, respectively. Using kinematic

relations, these components and the shear-strain rate $\dot{\varepsilon}_{rz}$ are expressed in terms of the velocity components as follows:

$$\dot{\varepsilon}_r = \frac{\partial u}{\partial r}, \qquad \dot{\varepsilon}_\theta = \frac{u}{r}, \qquad \dot{\varepsilon}_{rz} = \frac{\partial v}{\partial r}.$$

The medium is not deformed in the z direction ($\dot{\varepsilon}_z = 0$).

The stress state of the ST material is determined using plastic flow theory [13]. For the examined case of loading of an elastoplastic medium, the constitutive equations of this theory are written as

$$\begin{gathered}\frac{ds_z}{dt} + 2G\dot{\lambda}s_z = \frac{2G}{3\rho}\frac{d\rho}{dt}, \qquad \frac{ds_r}{dt} + 2G\dot{\lambda}s_r = 2G\Big(\dot{\varepsilon}_r + \frac{1}{3\rho}\frac{d\rho}{dt}\Big), \\ \frac{ds_\theta}{dt} + 2G\dot{\lambda}s_\theta = 2G\Big(\dot{\varepsilon}_\theta + \frac{1}{3\rho}\frac{d\rho}{dt}\Big), \qquad \frac{d\tau_{rz}}{dt} + 2G\dot{\lambda}\tau_{rz} = G\dot{\varepsilon}_{rz},\end{gathered} \tag{4}$$

where s_z, s_r, and s_θ are the normal components of the stress deviator, G is the shearing modulus of the medium, $\dot{\lambda}$ is a scalar factor, which is expressed in terms of the specific power of plastic deformation dA_p/dt and the yield strength of the medium σ_Y as follows:

$$\dot{\lambda} = \frac{3}{2\sigma_Y^2}\frac{dA_p}{dt}.$$

With allowance for the Mises–Schleicher plastic condition [5], which is usually employed to describe the plastic deformation of soils, the yield strength of the medium σ_Y was assumed to depend on the pressure acting in the medium p:

$$\sigma_Y(p) = \sigma_{Y0} + \psi p/(1 + \psi p/(\sigma_{Y\infty} - \sigma_{Y0})),$$

where σ_{Y0} is the shear strength of the soil at zero mean stresses (an analog of the initial cohesion of the medium in the Coulomb–Mohr condition [4]), ψ is an analog of the internal friction coefficient, and $\sigma_{Y\infty}$ is the ultimate shear strength of the medium as $p \to \infty$.

The normal stress-tensor components $\sigma_z = s_z - p$, $\sigma_r = s_r - p$, and $\sigma_\theta = s_\theta - p$ are determined from the quantities s_z, s_r, and s_θ calculated from (4) and the pressure p in the ST material.

In determining the pressure in the soil, we assumed that it depends only on the volumetric strain of the soil particles and the effect of their internal energy was ignored. The relation between volumetric strain and pressure was specified by the dynamic equation

$$\frac{\rho_0}{\rho} = \sum_{i=1}^{3} \alpha_i \Big(1 + \frac{p - p_0}{K_i}\Big)^{-1/n_i}, \tag{5}$$

where the quantities α_i characterize the phase composition of the ST material and correspond to the volume concentration of the pores occupied by air (α_1) and the liquid (α_2) and solid (α_3) components, ρ_0 is the density of the medium under normal conditions (pressure p_0), and K_i and n_i are experimental parameters [5]. The compressibility equation (5) was constructed under the assumption that the pressures in all three phase components are equal in any small volume. In this case, the compressibility of each phase is described by the Tait equations [5], and the total volumetric strain is defined as the sum of the volumetric strains of the individual components. For a known phase composition, the initial density of the soil ρ_0 is defined as $\rho_0 = \alpha_2\rho_{20} + \alpha_3\rho_{30}$, where $\rho_{20} = 1000$ kg/m^3, $\rho_{30} \approx 2600$–2700 kg/m^3 are the densities of the liquid and solid components.

The parameters K_i and n_i ($i = 1, 2, 3$) in (5) were taken from [5]. Thus, the volumetric compressibility of the soil material (5) is determined only by the phase composition of the soil, and in view of the obvious relation $\alpha_1 + \alpha_2 + \alpha_3 = 1$, to specify the compressibility law, it suffices to specify the volume concentrations of any two of the three components (usually, these are the parameters α_1 and α_2, which characterize the volume concentration of air pores and the liquid component).

Soils are characterized by the compactibility property after unloading, and the relationship between the pressure and density under unloading (pressure release) differs from that in the previous loading stage (pressure rise) [5]. However, in the examined problem of a soil loaded by an infinite cylindrical piston which expands at a constant velocity, there are no conditions for complete unloading of the soil in any region. Therefore, in specifying

TABLE 1

Characteristic of Soil Targets

ST material	α_1, %	ρ_0, kg/m^3	G, GPa	Ψ	σ_{Y0}, MPa	$\sigma_{Y\infty}$, MPa
Strong rock (ST1)	1	2620	10	1	100	150
Dense soil (ST2)	25	1990	0.05	0.5	5	15

the relationship between the volumetric strain and pressure for the entire process, we restrict ourselves only to Eq. (5).

Let us formulate the boundary conditions on the surface of the expanding piston $r = R$ (Fig. 1). The kinematic condition $u(R,t) = u_c$ specifies the radial velocity of the soil particles at the interface with the piston equal to the expansion velocity of the piston. The boundary condition defining the axial motion of the soil is a dynamic type condition and has the form

$$\tau_{rz}(R,t) = \tau_n, \tag{6}$$

where τ_n are the contact shear stresses on the piston surface. In the presence of dry friction on the piston surface, these stresses are related to the contact normal stresses $\sigma_r(R,t)$ via the skin-friction coefficient μ: $\tau_n = \mu|\sigma_r(R,t)|$ [this relationship takes place when the radial stresses on the piston surface are compressing, i.e., $\sigma_r(R,t) < 0$; otherwise, $\tau_n = 0$].

Obviously, condition (6) remains valid until the axial velocity of the soil particles at the interface with the piston $v(R,t)$ becomes equal to the axial velocity of the piston v_c, after which the value $v(R,t)$ can no longer increase. Thus, in using condition (6), one should additionally verify the inequality $v(R,t) < v_c$ and if it is not satisfied, condition (6) should be replaced by the kinematic boundary condition $v(R,t) = v_c$.

The initial values of all required parameters of motion and state of the ST were specified assuming that the soil is not perturbed and is at rest at the initial time ($t = 0$).

Calculation Results. For the formulated model, the evolution of the parameters of motion and state of the soil with time were determined using a numerical finite-difference method based on the Wilkins method [14] and the results of [12]. The calculations were performed for STs [5] with strongly different strength properties — a strong rock (ST1) and a dense soil (ST2). The characteristics of the STs are listed in Table 1 (it was assumed that a liquid component is absent in both STs). The axial velocities of the piston v_c were 250, 500, and 1000 m/sec. For each value of the axial velocity, three values of the radial expansion velocity of the piston u_c were considered, so that their ratios u_c/v_c were 0.25, 0.5 and 1.0 (within the framework of the hypothesis of plane cross sections [2], this choice corresponds to projectile cone angles 2γ of 29, 53, and 90°, respectively).

As regards the choice of the initial radius R_0 of the expanding piston in the model considered, the following considerations are relevant. It cannot be set equal to zero because in this case the presence of the radial velocity for the soil particles on the symmetry axis ($r = 0$) makes the problem singular at the initial time (for $r = 0$, for example, the strain-rate-tensor components $\dot{\varepsilon}_r$ and $\dot{\varepsilon}_\theta$ become undetermined. It is also clear that immediately in the vicinity of the projectile nose tip, the employed model of loading of a medium by an infinite cylindrical piston is far from reality (the nature of motion of the medium in this region due to projectile penetration corresponds more to its loading by a spherical piston). Thus, this model provides reliable predictions only at a distance from the cone tip (one of the factors determining this distance is, for example, the rounding radius of the conical nose tip, which is always inherent in real projectiles).

In view of the foregoing, it is reasonable not to specify the quantity R_0 and to use it if necessary as a scaling parameter in determining the various characteristics of ST loading by the expanding piston. With such an approach to the representation of the numerical-simulation results, they do not depend on the choice of R_0 and are applicable for projectiles of any dimensions.

Projectile penetration into a ST generates a shock wave whose parameters are determined by the radial velocity of piston expansion. Figure 2 shows the radial-stress distributions in ST1 and ST2 for various current expansion radii R/R_0 of a piston at $u_c = 500$ m/sec. Of special practical interest is the variation in the radial stress $\sigma_r(R)$ on the piston surface (this variation provides an insight into the evolution of the normal stresses σ_n at the interface between the projectile and ST). In Fig. 2, the radial stresses on the piston surface for various piston expansion radii are shown by open points. It is evident that the radial stresses on the piston are maximal at the

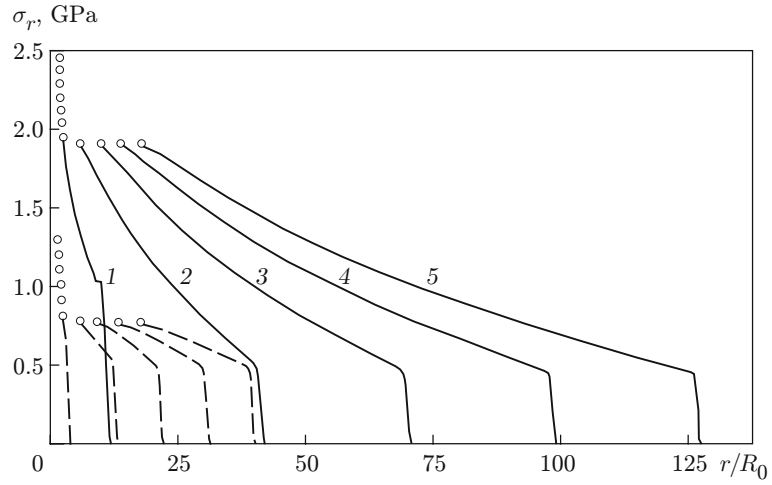

Fig. 2. Radial-stress distributions in ST1 (solid curves) and ST2 (dashed curves) for a piston expansion velocity $u_c = 500$ m/sec and expansion radii $R/R_0 = 2$ (curve 1), 6 (curve 2), 10 (curve 3), 14 (curve 4), and 18 (curve 5); the open points refer to the radial stresses on the piston surface.

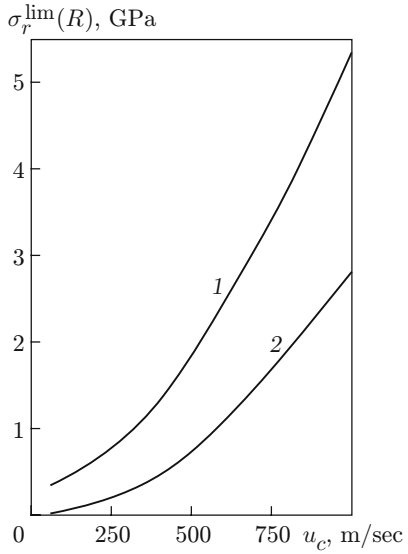

Fig. 3. Radial stresses on the piston surface versus piston expansion velocity: curves 1 and 2 refers to ST1 and ST2, respectively.

initial moment of its expansion (when the piston impacts the media to generate a shock wave in it). Subsequently, the stresses rapidly decrease and, what is especially important, reach a constant level that hardly depends on the piston expansion radius (see Fig. 2). The time from the beginning of piston expansion after which the value of $\sigma_r(R)$ remains almost unchanged corresponds to an increase in the piston radius by only $1-2\,R_0$. In the examined range of kinematic parameters of the piston, the effect of the axial velocity of the piston v_c on the value of $\sigma_r(R)$ is insignificant, so that the steady-state value of the radial stresses on the piston $\sigma_r^{\lim}(R)$ is completely determined by its radial velocity. The dependence of this steady-state value on the velocity u_c is parabolic for various ST (Fig. 3). This agrees qualitatively with the empirical resistance laws [6], which are widely used to determine the normal stresses on the projectile surface during penetration into STs. From the results obtained for the model considered, it follows that the normal stresses in the vicinity of the projectile tip can far exceed the stresses on the remaining segments of its surface (the initial stage of piston expansion in Fig. 2).

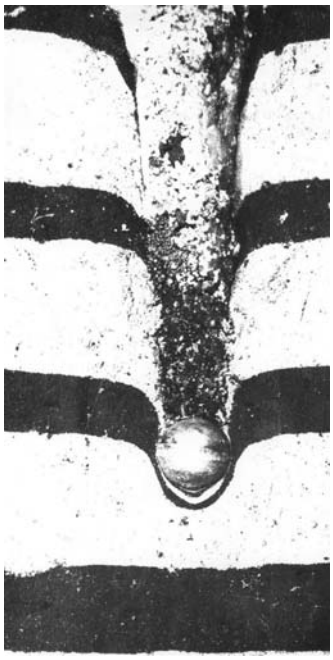

Fig. 4. Section of a cavity in a sand target for penetration of a spherical projectile.

As regards the shear motion of the material ST (motion along the z axis, see Fig. 1), the calculations gave the following results. For almost all penetration conditions considered, an attachment regime occurs at the interface between the expanding piston with the soil — a soil layer adjacent to the piston is set in motion in the axial direction (the calculations were performed for the minimum friction coefficient on the piston surface $\mu = 0.2$). The thickness of this layer, remaining smaller than the current piston expansion radius, increases linearly with increase in the latter (as the thickness h_s of the layer of shear motion we used the distance from the piston at which the axial velocity of the media decreased to 10% of its axial velocity at the interface).

The growth rate of the shear-layer thickness increases with an increase in the strength properties of the ST [15]. For a piston expansion radius $R/R_0 = 20$, the characteristic value of h_s is a few R_0 for ST1 and a few tenths of R_0 for ST2. In the calculations, the regime of axial sliding of the ST material at the interface with the piston was observed only at piston-expansion velocities $u_c \approx 100$ m/sec or lower. In this case, the boundary of the medium did not completely stopped but continued to move in the axial direction behind the piston at a lower velocity than the piston velocity.

The calculated effect of setting a thin soil layer at the interface in axial motion by a piston agrees with experimental data for projectile penetration into STs. Figure 4 shows a section of a specially prepared sand target (consisting of layers of contrast color) penetrated by a spherical projectile. One can see how the target layers are stretched behind the projectile along the boundaries of the cavity.

Figure 5 shows shear-stress distributions in ST1 and ST2 for various piston expansion radii R/R_0, $v_c = 500$ m/sec, and $u_c = 500$ m/sec. It is evident that the shear stresses are also localized in a thin layer of the ST at the interface with the piston. In the initial stage of piston expansion, the value of the shear stresses at the interface (which determines one of the resistance force components during penetration) increases slightly for a short time, after which it remains almost unchanged and is approximately half the shear strength of the ST material that corresponds to the pressure acting on the interface (in Fig. 5, the contact shear stresses for various piston expansion radii are shown by open points; for the chosen scales of representation of shear stresses in these STs, the curves for ST1 and ST2 coincide). For the STs used in the calculations, the ultimate shear strengths (for $p \to \infty$) differed by a factor of 10 (see Table 1) and the contact shear stresses (Fig. 5) differed by the same magnitude. The pressure acting on the interface ensured that the strength properties of both STs were close to their ultimate values. For various penetration conditions (with the entrainment of the soil layer by the piston), the difference between the

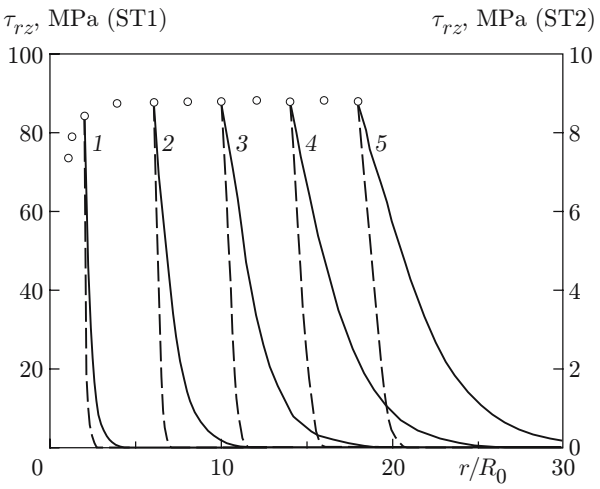

Fig. 5. Shear-stress distributions in ST1 (solid curves) and ST2 (dashed curves) for $u_c = 500$ m/sec, $v_c = 500$ m/sec, and piston expansion radii $R/R_0 = 2$ (curve 1), 6 (curve 2), 10 (curve 3), 14 (curve 4), and 18 (curve 5); the open points refer to contact shear stresses.

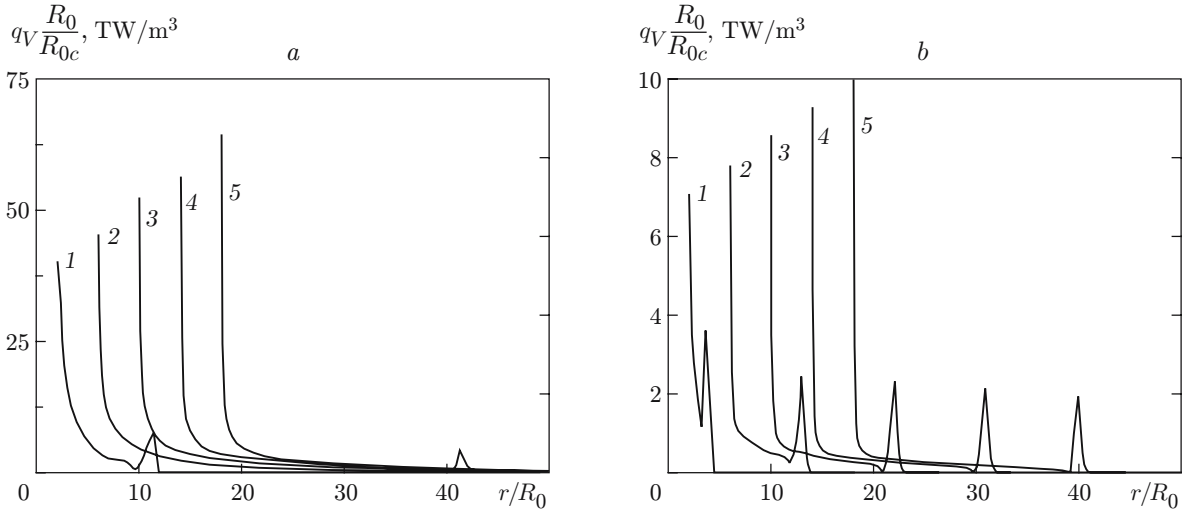

Fig. 6. Distributions of volumetric heat release in ST1 (a) and ST2 (b) for $u_c = 500$ m/sec, $v_c = 500$ m/sec, and piston expansion radii $R/R_0 = 2$ (curve 1), 6 (curve 2), 10 (curve 3), 14 (curve 4), and 8 (curve 5).

shear stresses on the piston surface and the value of $\sigma_Y/2$ was in the range of 20–30%. It should be noted that beginning even with a piston expansion velocity of 150 m/sec, the shear stresses τ_n acting on its surface are far below the value of $\mu\sigma_r(R)$ determined using the dry friction law.

During loading of a ST by a piston which expands and moves axially, there is intense plastic deformation of the ST material. This process is accompanied by dissipation of plastic strain energy, which should result in a considerable heat release in the medium. Figure 6 gives distributions of the volumetric heat release q_V in ST1 (Fig. 6a) and ST2 (Fig. 6b) for various piston expansions radii R/R_0 at $v_c = 500$ m/sec and $u_c = 500$ m/sec. In Fig. 6, to take into account the scale effect of the problem, which is determined by the initial piston radius q_V, we multiply the value of R_0 by the dimensionless ratio R_0/R_{0c}, where R_{0c} is a constant which has the dimension of length and is set equal to 1 mm (to obtain the absolute value of the heat release q_V for a given R_0, one needs to divide the data in Fig. 6 by the value of R_0 in millimeters). The heat-release peak moving in the medium corresponds to the shock-wave front but especially intense heat release occurs in a soil layer in contact with the

piston (Fig. 6). This is due to the intense shear deformation of the soil particles in the layer of axial motion at the interface with the piston. As the piston expands, the volumetric heat-release power at the interface increases — the radial compression of the soil particles leads to an increase in the nonuniformity of the radial distribution of their axial velocity at the interface with the piston and, hence, to an increase in their shear strain rate. The value of v_c at the interface increases almost linearly with an increase in the axial velocity of the piston q_V.

Thus, the absence of soil sliding at the interface eliminates the frictional mechanism of heat release with an improbably strong thermal effect on the penetrating projectile. Because of the entrainment of the ST layer in contact with the projectile, the heat release is transferred from the interface into the bulk of the medium, replacing internal skin friction as the heat source. With this mechanism of thermal effect, the thermal load on the penetrating projectile is apparently much lower than that for the frictional heating of its surface. The temperature of the medium at the interface with the projectile cannot grow without bound. Its growth is limited by the phase-transition temperature of the ST material, approaching which the strength properties of the soil decrease and, accordingly, the internal friction vanishes.

For the heat release q_V corresponding to an axial velocity of about 500 m/sec, the growth rate of the soil temperature at the piston surface $\Delta T_s/\Delta t = q_V/(\rho c)$ (c is the heat capacity of the ST material) provides a temperature rise ΔT_s of up to 80 K for ST1 and up to 10–14 K for ST2 during the time of axial displacement of the piston by the value of R_0. Such heating rates should lead to fast thermal softening of the ST layer in contact to the projectile and, hence, to a decrease in the shear stresses at the interface (whose value, as noted above, is determined by the strength properties of the ST material). With a loss of the strength properties of the boundary layer of the ST due to strong heating, viscous properties may begin to play an important role, and this requires a separate consideration.

REFERENCES

1. W. A. Allen, E. B.Mayfield, and H. L. Morrison, "Dynamics of a projectile penetrating sand," *J. Appl. Phys.*, **28**, No. 3, 370–376 (1957).
2. A. Ya. Sagomonyan, *Penetration* [in Russian], Izd. Mosk. Gos. Univ., Moscow (1974).
3. V. A. Veldanov, A. L. Isaev, and Yu. M. Pushilin, "Effect of volumetric unloading of soil on cavity formation during projectile penetration," in: *Proc. XXIII Conf. on Numerical Methods of Solving Elastic and Plastic Problems*, Inst. of Theor. and Appl. Mech., Novosibirsk (1995), pp. 36–40.
4. S. S. Grigor'yan, "On the main concepts of soil dynamics," *Prikl. Mat. Mekh.*, **24**, No. 6, 1057–1072 (1960).
5. A. A. Vovk, B. V. Zamyshlyaev, L. S. Evterev, et al., *Soil Behavior under Pulsed Loading* [in Russian], Naukova Dumka, Kiev (1984).
6. V. A. Veldanov, "Resistance to projectile penetration into soil," *Oboron. Tekh.*, **4**, 32–34 (1995).
7. M. M. Aleksandrov, *Resistance to Motion of Tubes in a Wellbore* [in Russian], Nedra, Moscow (1978).
8. V. A. Veldanov, V. E. Smirnov, and S. V. Fedorov, "High-velocity penetrator for deep sounding of a soil," in: *Dvoinye Tehhnol.*, No. 2, 11–15 (2000).
9. O. V. Pereverzeva and V. A. Balakin, "Heat distribution between bodies in friction," *Trenie Iznos*, **13**, No. 3, 507–516 (1992).
10. V. E. Alemasov, A. F. Dregalin, and A. P. Tishin, *Theory of Rocket Engines* [in Russian], Mashinostroenie, Moscow (1989).
11. A. V. Lykov, *Heat-Conduction Theory* [in Russian], Vysshaya Shkola, Moscow (1967).
12. A. L. Isaev and V. V. Selivanov, "Numerical implementation of the physical relations for a strengthening elastoplastic medium," *Probl. Prochn.*, No. 5, 47–49 (1989).
13. A. A. Il'yushin, *Continuum Mechanics* [in Russian], Izd. Mosk. Gos. Univ., Moscow (1990).
14. M. L. Wilkins, "Calculation of elastic-plastic flow," in: *Methods in Computational Physics*, Academic Press, New York (1964), pp. 211–263.
15. S. V. Fedorov and V. A. Veldanov, "Formation of a boundary layer during penetration of a rigid projectile into soil," in: *Vth Khariton Scientific Readings*, Proc. Int. Conf., Inst. of Exp. Phys., Sarov (2003), pp. 491–495.